We are IntechOpen, the world's leading publisher of Open Access books Built by scientists, for scientists

6,900
Open access books available

185,000
International authors and editors

200M
Downloads

Our authors are among the

154
Countries delivered to

TOP 1%
most cited scientists

12.2%
Contributors from top 500 universities



WEB OF SCIENCE™

Selection of our books indexed in the Book Citation Index in Web of Science™ Core Collection (BKCI)

Interested in publishing with us?
Contact book.department@intechopen.com

Numbers displayed above are based on latest data collected.
For more information visit www.intechopen.com



Chapter

Single-Atom Field-Effect Transistor

Er'el Granot

Abstract

A simple single-atom transistor configuration is suggested. The transistor consists of only a nanowire, a single-point impurity (the atom), and an external capacitor. The transistor gate is controlled by applying a transverse voltage on the capacitor. The configuration does not rely on tunneling current and, therefore, is less sensitive to manufacturing processes since it requires less accuracy and fewer production processes. Moreover, unlike resonant-tunneling devices, the proposed transistor configuration does not suffer from a compromise between high speed and high extinction ratio. In fact, it is shown that this transistor can be extremely fast, without affecting the signal's extinction ratio, which can be as high as 100%.

Keywords: quantum dots, quantum point defect, point impurity, quantum transistor, single-atom transistor, field-effect transistor

1. Introduction

Despite the fact that the field-effect transistor (FET) was patented long before the formal invention of the transistor by Lilenfeld (in 1926) and Heil (in 1934), it was produced only two decades later when its patent expired. Nevertheless, its benefits were soon realized, and it became the building block of every integrated chip.

In 1975, Gordon Moore made a bold statement, which he updated a decade later, that the number of transistors on an integrated chip doubles every couple of years [1, 2]. This Moore's law is surprisingly still valid. In fact, it seems that this is the only parameter, which keeps growing exponentially for five consecutive decades. A simple extrapolation of this trend reveals that within a decade, the size of the average transistor should be no larger than the dimensions of a single atom.

The idea to manufacture few atom-based electronic devices was first suggested by Richard Feynman, but it has become a reality only after the scanning tunneling microscope (STM) was invented, and manipulations of single atoms became feasible [3].

Recently there have been several attempts to fabricate nano-devices, which are based on several atoms and even on a single atom [4–9]. These devices can operate as single-atom transistors [10–13]. The main problem with these devices is that while the device's core is based on a single atom, the connectors are considerably larger, and consequently, it is extremely complicated to model the device since the models are spread over several length scales.

In order to simplify the model, the atom and the leads should both be presented in the simplest form possible.

That was the main motivation to create a model, in which the entire transistor is within the leads [14]. This configuration is in high agreement with the experiment of a single-atom transistor [10] and, at the same time, can be simulated by a relatively simple model. The solutions of this model can be expressed, with great accuracy, by analytical expressions.

However, since this configuration is based on quantum tunneling, the single atom is not directly connected to the conducting leads (for resonant tunneling via a point defect without the insulators, see [15, 16]). Such a device is very difficult to manufacture, since the atom has to be encapsulated by the surrounding (other) atoms; it has to be located with great accuracy, and due to the resonant nature of the device, the atom must be located exactly at the center of the device; otherwise, the device's efficiency exponentially decreases.

However, resonant tunneling is not essential to achieve fine control. For example, it has been shown that a single-point defect in a nanowire can be a perfect reflector for certain energies. Moreover, the point defect can cause a universal conduction reduction. At certain Fermi energies, the conductance drops at exactly $2e^2/h$ [17].

Since the energy level of the point defect's bound state can be modified, then a simple nanowire with a single defect (a single atom) can be used as a nanotransistor. This is a much simpler device, which can be produced in fewer production stages than resonant-tunneling devices.

However, to control the resonance energy of the point defect, an external electric field should be applied. The field affects the entire device and does not selectively influence only the defect. Therefore, there is a need for a complete model, which integrates the nanowire, the point defect, and the electric field.

The object of this chapter is to present such a model of a nanotransistor, which is governed not by resonant-tunneling process but by Fano anti-resonance [18], which is generated by the interaction between the point defect and the nanowire. In this transistor configuration, the FET's gate is controlled by an external electric field.

2. The model

The system is presented in **Figure 1**. The system consists of an infinite nanowire (in the longitudinal x-direction), whose width (in the transverse y-direction) is w, a point defect, whose distance from the boundary of the nanowire is $w\varepsilon$, and an external capacitor, whose voltage and charge can be controlled by a power source.

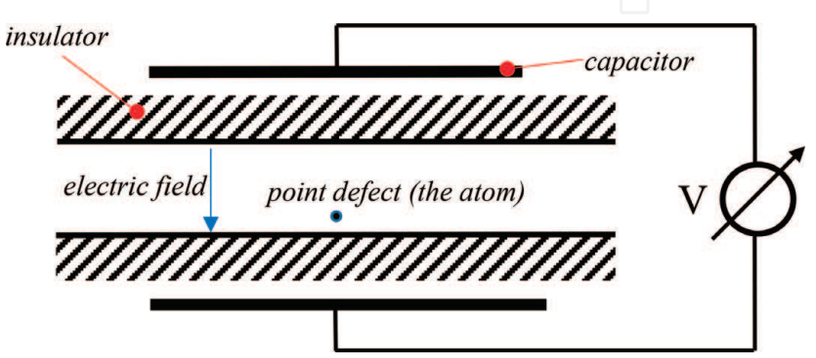


Figure 1.
Model schematic. The capacitor creates the transverse electric field, and the point defect simulates the single atom.

Mathematically, the model can be described by the 2D stationary Schrödinger equation

$$\frac{\partial^2\psi}{\partial x^2}+\frac{\partial^2\psi}{\partial y^2}+(E-U(y)+Fy)\psi=-D(\mathbf{r}-\mathbf{r_0})\psi \tag{1}$$

in which normalized units (where Planck constant is $\hbar=1$ and the electron's mass is $m=1/2$) were used. In this equation

$$U(y)=\begin{cases}0 & 0<y<w\\ \infty & else\end{cases} \tag{2}$$

is the boundaries' potential, which confines the dynamics to the wire's geometry. F is the electric field.

The point defect, which models the single atom, is presented by the asymmetric impurity D function (IDF) [19–21]

$$D(\mathbf{r})\equiv\lim_{\rho\to0}\frac{2\sqrt{\pi}\delta(y)\exp\left(-x^2/\rho^2\right)}{\rho\ln\left(\rho_0/\rho\right)} \tag{3}$$

which is located at $\mathbf{r}_0=\hat{y}\varepsilon$, and ρ_0 is related to the impurity's bound eigenenergy by

$$E_0=-\frac{16\exp\left(-\gamma\right)}{\rho_0^2}\cong-\frac{8.98}{\rho_0^2} \tag{4}$$

where $\gamma\cong0.577$ is Euler constant [22]. On the other hand, the relation between ρ_0 and the physical properties of a real physical impurity (which has a finite radius a and a finite local potential V_0) is

$$\rho_0=2a\exp\left(\frac{2}{V_0a^2}+\frac{\gamma}{2}\right). \tag{5}$$

The homogeneous eigenstates solutions of the wire, i.e., solutions without the point defect, are

$$\psi_{n,E}(x,y)=\exp\left(ik_nx\right)\chi_n(y) \tag{6}$$

where $\chi_n(y)$ are the eigenstates of the one-dimensional differential equation

$$\frac{\partial^2\chi_n(y)}{\partial y^2}+(E_n-U(y)+Fy)\chi_n(y)=0 \tag{7}$$

with the corresponding eigenvalues

$$k_n^2=E-E_n. \tag{8}$$

These eigenstates can be written using the Airy functions Ai and Bi [22] and the normalized parameter

$$\xi\equiv yF^{1/3}+\left(E-k_n^2\right)/F^{2/3}=F^{1/3}\left\{y+\left(E-k_n^2\right)/F\right\}$$

as

$$\chi_n(\xi) = N\{Ai(\xi)Bi(\xi_0) - Ai(\xi_0)Bi(\xi)\} \tag{9}$$

where N is the normalization constant, $\xi_0 \equiv F^{1/3}\{E_n/F\}$, where the eigenvalues E_n are determined by the infinite solutions of the transcendental equation.

$\chi_n(\xi_w) = 0$, when $\xi_w \equiv F^{1/3}\{w + E_n/F\}$.

In the case of a weak electric field, the eigenstates can be written to a first order in the electric field as a superposition of the *free* (zero electric field) eigenstates

$$\phi_m(y) = \sqrt{\frac{2}{w}}\sin(m\pi y/w) \tag{10}$$

namely,

$$\chi_m(y) = \phi_m(y) + Fw^3 \sum_q \phi_q(y) \frac{(-1)^{m+q} - 1}{2} \frac{mq}{(m+q)^3(m-q)^3} \frac{8}{\pi^4} \tag{11}$$

with the corresponding eigenenergies (again to the first order in F)

$$E_n \cong (n\pi/w)^2 + \frac{1}{2}Fw. \tag{12}$$

Clearly, in the absence of the point defect (the atom), there is no coupling between the transverse direction and the longitudinal one, i.e., the capacitor cannot affect the longitudinal conductance.

There is an exception, of course, if the capacitor occupies a finite region in space, in which case the electric field does create a coupling between the modes. But in the regime of a weak electric field, this coupling a_{mq} is also very weak

$$a_{mq} = Fw^3 \frac{(-1)^{m+q} - 1}{2} \frac{mq}{(m+q)^3(m-q)^3} \frac{8}{\pi^4}. \tag{13}$$

Even to adjacent modes (where most of the energy is transferred), the coupling is very weak

$$a_{m,m\pm1} = \mp Fw^3 \frac{m(m \pm 1)}{(2m \pm 1)^3} \frac{8}{\pi^4} \tag{14}$$

For example, the coupling between the first and the second modes is as small as $a_{1,2} \cong 0.0061Fw^3$.

However, the presence of the point defect breaks the Cartesian symmetry and increases the coupling between the modes.

The general solution, which takes the point defect into account, is

$$\psi(\mathbf{r}) = \psi_{inc}(\mathbf{r}) - \frac{G^+(\mathbf{r}, \mathbf{r}_0)\psi_{inc}(\mathbf{r}_0)}{1 + \int d\mathbf{r}' G^+(\mathbf{r}', \mathbf{r}_0) D(\mathbf{r}' - \mathbf{r}_0)} \int d\mathbf{r}' D(\mathbf{r}' - \mathbf{r}_0) \tag{15}$$

where $\psi_{inc}(\mathbf{r})$ is the incoming wavefunction, which can be chosen as one of the eigenmodes $\chi_n(y)$, which in the case of a weak electric field can be approximated by Eq. (11) (or Eq. (10), i.e., by $\phi_m(y)$); $G^+(\mathbf{r}, \mathbf{r}_0)$ is the outgoing 2D Green function, i.e., $G^+(\mathbf{r}, \mathbf{r}_0)$ is the solution of the partial differential equation

$$-\nabla^2 G^+(\mathbf{r}, \mathbf{r}_0) + [U(y) - E - Fy]G^+(\mathbf{r}, \mathbf{r}_0) = -\delta(\mathbf{r} - \mathbf{r}_0) \tag{16}$$

which can be written in terms of the 1D eigenstates $\chi_m(y)$ as

$$G(\mathbf{r},\mathbf{r}') = \sum_{n=1}^{\infty} \frac{\chi_n(y)\chi_n^*(y')}{2i\sqrt{E-E_n}} \exp\left(i\sqrt{E-E_n}|x-x'|\right). \tag{17}$$

The scattered solution is therefore

$$\psi(\mathbf{r}) = \exp(ik_n x)\chi_n(y) - \sum_{m=1}^{\infty} A_{n,m}\chi_m(y)\exp(ik_m|x|) \tag{18}$$

with the coefficients

$$A_{n,m} \equiv \lim_{\rho\to 0} \frac{\frac{\chi_n(\varepsilon)\chi_m^*(\varepsilon)}{2ik_m}}{\frac{\ln(\rho_0/\rho)}{2\pi} + \sum_{q=1}^{\infty} \frac{\chi_q(\varepsilon)\chi_q^*(\varepsilon)}{2ik_q}\exp\left(-\left|E-E_q\right|\rho^2/4\right)}. \tag{19}$$

The transmitted solution ($x > 0$) is thus

$$\psi(\mathbf{r}) = \sum_{m=1}^{\infty} \exp(ik_m x)\chi_m(y)\{\delta_{n,m} - A_{n,m}\}. \tag{20}$$

Eq. (18) is a generic solution; however, there are two types of energies, for which the solution reveals a universal pattern.

3. Universal transition patterns

When the particle's energy is equal exactly to one of transverse eigenenergies, i.e., when $E \to E_{Q,}$ then the wavefunction reduces to a simple but *universal* expression

$$\psi(\mathbf{r}) = \sum_{m=1}^{\infty} \exp(ik_m x)\chi_m(y)\left\{\delta_{n,m} - \delta_{Q,m}\frac{\chi_n(\varepsilon)}{\chi_Q(\varepsilon)}\right\} = \exp\left(i\sqrt{E_Q - E_n}x\right)\chi_n(y) - \chi_Q(y)\frac{\chi_n(\varepsilon)}{\chi_Q(\varepsilon)}. \tag{21}$$

A similar universality was shown for zero-field wire [23] (for other patterns, see [24])

$$\psi(\mathbf{r}) = \exp\left(i\pi\sqrt{Q^2-n^2}x\right)\sin\left(\frac{n\pi y}{w}\right) - \sin\left(\frac{Q\pi y}{w}\right)\frac{\sin(n\pi\varepsilon/w)}{\sin(Q\pi\varepsilon/w)}, \tag{22}$$

but Eq. (21) solution is valid in the presence of an electric field as well.

This solution is universal in the sense that it is totally independent of the point defect's strength (potential), which is manifested by the parameter ρ_0—a parameter that does not appear in Eq. (21). This pattern is presented in the upper panel of **Figure 2**.

Clearly, when the defect is close to the surface, i.e., $\varepsilon/w << 1$, then the solution is even independent of ε

$$\psi(\mathbf{r}) \cong \exp\left(i\pi\sqrt{Q^2-n^2}x\right)\sin\left(\frac{n\pi y}{w}\right) - \sin\left(\frac{Q\pi y}{w}\right)\frac{n}{Q}. \tag{23}$$

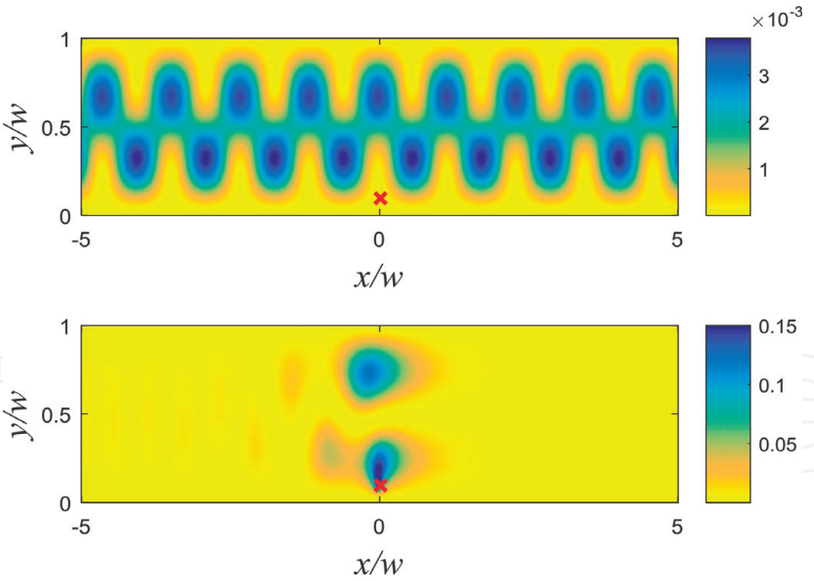


Figure 2.
A false color presentation of the conductance pattern. The spatial distribution in the wire of the probability density $|\psi(\boldsymbol{r})|^2$ is plotted at the transition energy $E = E_2 \cong (2\pi/w)^2 + Fw/2$ (upper panel) and at the zero-current energy $E = E_2^{\min}$ (lower panel). The crosses represent the point defect's location.

At this operation point, the transistor experiences maximum transmission with maximum current, which is universal and is independent of the point defect parameters. The defect deforms the conducting pattern, but it does not transfer any current to the mth mode. Consequently, the current remains in the initial nth mode, as if the defect is absent.

4. Universal conductance reduction

Another important case, which is going to be relevant to the transistor operation, occurs below the next energy transition where there is a dip in the transmission coefficient, and the conductance decreases by exactly $2e^2/h$.

Let the incoming particle energy be within the energy range $E_{Q-1} < E < E_Q$; for which case it is convenient to split the denominator of the coefficient, i.e., to rewrite Eq. (19) as

$$A_{n,m} \equiv \lim_{\rho\to 0} \frac{\frac{\chi_n(\varepsilon)\chi_m^*(\varepsilon)}{ik_m}}{\frac{\ln(\rho_0/\rho)}{\pi} + \sum_{q=1}^{Q-1} \frac{\chi_q(\varepsilon)\chi_q^*(\varepsilon)}{i\sqrt{E-E_q}} - \frac{\chi_Q(\varepsilon)\chi_Q^*(\varepsilon)}{\sqrt{E_Q-E}} - \sum_{q=Q+1}^{\infty} \frac{\chi_q(\varepsilon)\chi_q^*(\varepsilon)}{\sqrt{E_q-E}} \exp\left(-|E-E_q|\rho^2/4\right)} \tag{24}$$

or

$$A_{n,m} \equiv \frac{\frac{\chi_m^*(\varepsilon)\chi_n(\varepsilon)}{i\sqrt{E-E_m}}}{\frac{\ln(\rho_0/R(\varepsilon))}{\pi} + \sum_{q=1}^{Q-1} \frac{\chi_q(\varepsilon)\chi_q^*(\varepsilon)}{i\sqrt{E-E_q}} - \frac{\chi_Q(\varepsilon)\chi_Q^*(\varepsilon)}{\sqrt{E_Q-E}}}, \tag{25}$$

where

$$\ln R(\varepsilon) \equiv \lim_{\rho\to 0}\left[\ln\rho + \pi \sum_{q=Q+1}^{\infty} \frac{\chi_q(\varepsilon)\chi_q^*(\varepsilon)}{\sqrt{E_q-E}} \exp\left(-|E-E_q|\rho^2/4\right)\right]. \tag{26}$$

The device's conductance can be evaluated as ([25, 26])

$$G = \frac{1}{\pi} \sum_{m,\, l<n} T_{ml}, \tag{27}$$

where

$$T_{n,m} = |\delta_{n,m} - A_{n,m}|^2 \frac{k_m}{k_n} = \begin{cases} |1 - A_{n,n}|^2 & n = m \\ |A_{n,m}|^2 \dfrac{k_m}{k_n} & n \neq m \end{cases} \tag{28}$$

are the transmission coefficients (from the nth to the mth modes) of the wire with the impurity.

At the transition points, i.e., when $E = E_Q$ ($k_Q = 0$), the conductance is exactly

$$G = \frac{1}{\pi}(Q - 1), \tag{29}$$

which is $G = 2\frac{e^2}{h}(Q-1)$ in ordinary physical units.

On the other hand, at the minimum transmission point ($E = E_Q^{\min} < E_Q$), when the real part of the denominator of Eq. (25) vanishes, i.e., when

$$\frac{\ln(\rho_0/R(\varepsilon))}{\pi} = \frac{\chi_Q(\varepsilon)\chi_Q^*(\varepsilon)}{\sqrt{E_Q - E_Q^{\min}}}, \tag{30}$$

then

$$A_{n,m} \equiv \frac{\frac{\chi_m^*(\varepsilon)\chi_n(\varepsilon)}{i\sqrt{E-E_m}}}{\sum_{q=1}^{Q-1} \frac{\chi_q(\varepsilon)\chi_q^*(\varepsilon)}{i\sqrt{E-E_q}}} = \frac{1}{\frac{\sqrt{E-E_m}}{\chi_m^*(\varepsilon)\chi_n(\varepsilon)} \sum_{q=1}^{Q-1} \frac{\chi_q(\varepsilon)\chi_q^*(\varepsilon)}{\sqrt{E-E_q}}} = \frac{1}{\frac{k_m}{\chi_m^*(\varepsilon)\chi_n(\varepsilon)} \sum_{q=1}^{Q-1} \frac{\chi_q(\varepsilon)\chi_q^*(\varepsilon)}{k_q}}. \tag{31}$$

Using the definition

$$\sigma \equiv \sum_{q=1}^{Q-1} \frac{\chi_q(\varepsilon)\chi_q^*(\varepsilon)}{\sqrt{E - E_q}} = \sum_{q=1}^{Q-1} \frac{\chi_q(\varepsilon)\chi_q^*(\varepsilon)}{k_q} \tag{32}$$

the conductance $G = \frac{1}{\pi} \sum_{n,\, m<Q} |\delta_{n,m} - A_{n,m}|^2 \frac{k_m}{k_n}$ is equal exactly to

$$G = \frac{1}{\pi} \sum_{n,\, m<Q} \left| \delta_{n,m} - \frac{\chi_m^*(\varepsilon)\chi_n(\varepsilon)}{k_m \sigma} \right|^2 \frac{k_m}{k_n} = \frac{1}{\pi} \sum_{n,\, m<Q} \left[\delta_{n,m} - 2\frac{\chi_m^*(\varepsilon)\chi_n(\varepsilon)}{k_m \sigma} + \left| \frac{\chi_m^*(\varepsilon)\chi_n(\varepsilon)}{k_m \sigma} \right|^2 \right] \frac{k_m}{k_n} = \frac{Q-2}{\pi} \tag{33}$$

which is $G = 2\frac{e^2}{h}(Q-2)$ in ordinary physical units.

Therefore, there is exactly a one unit of conductance reduction between the transition energy E_Q and the minimum point just below it $E_Q^{\min}$

$$\Delta G = G(E_Q) - G\left(E_Q^{\min}\right) = \pi^{-1}, \tag{34}$$

which is $2e^2/h$ in ordinary physical units.

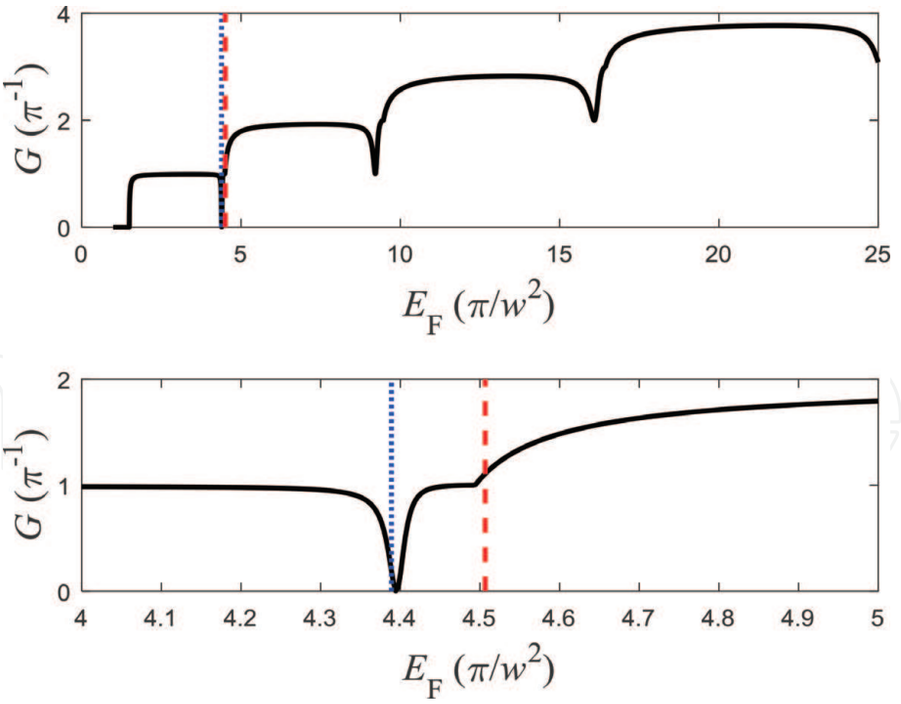


Figure 3.
The nanowire's conductance as a function of the particles' Fermi energy. The lower panel is a magnification of the transition zone. The dashed perpendicular line stands for the transition energy formula (Eq. (12)) $E = E_2$, and the dotted line corresponds to the zero-current energy formula (Eq. (30)) $E = E_2^{\min}$.

This result is a generalization of [17]. The probability density at the point of minimum conductance is presented in the lower panel of **Figure 2**, and the dependence of the conductance on the particles' Fermi energy is presented in **Figure 3**. The minima are clearly seen.

Moreover, the approximate analytical expressions of the transition energy Eq. (12) and the minimum energy Eq.(30) are presented by horizontal lines.

5. Zero transmission point

The current can vanish only when the Fermi energy is within the energy range $\pi^2/w^2 < E_F < 4\pi^2/w^2$, in which case only the first mode is propagating. The transmission of the first mode is

$$t_{1,1} = 1 - \left\{1 + \frac{i\sqrt{E_2 - E_1}}{|\chi_1(\varepsilon)|^2}\left[\frac{\ln(\rho_0/R(\varepsilon))}{\pi} - \frac{|\chi_2(\varepsilon)|^2}{\sqrt{E_2 - E}}\right]\right\}^{-1}, \tag{35}$$

in which case the zero-current energy is approximately

$$E_R \cong E_2 - \frac{\pi^2|\chi_2(\varepsilon)|^4}{\ln^2(\rho_0/R(\varepsilon))} \tag{36}$$

and in the case of weak fields, it can be written

$$t_{1,1} = 1 - \left\{1 + \frac{i\pi\sqrt{3}}{2\sin^2(\pi\varepsilon/w)}\left[\frac{\ln(\rho_0/R(\varepsilon))}{\pi} - \frac{2\sin^2(2\pi\varepsilon/w)}{w\sqrt{(2\pi/w)^2 + \frac{1}{2}Fw - E}}\right]\right\}^{-1} \tag{37}$$

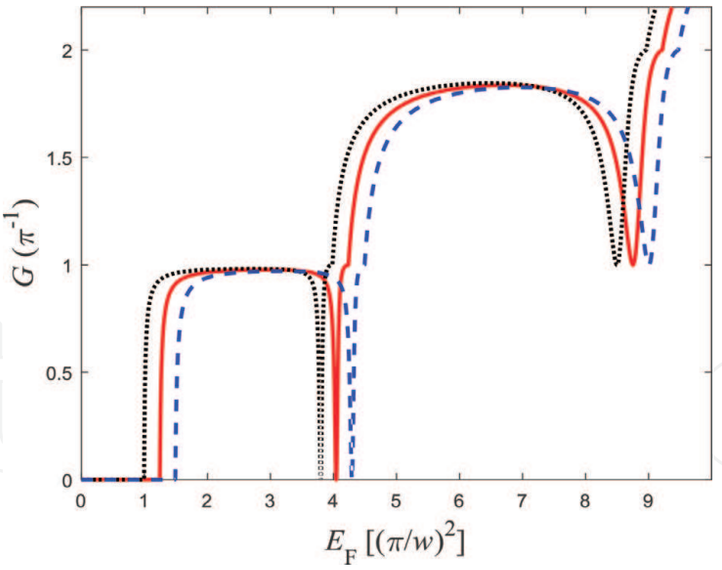


Figure 4.
The dotted curve stands for $Fw^3 = 0$; the solid curve stands for $Fw^3 = 5$; and the dashed curve stands for $Fw^3 = 10$.

with the zero-current (zero transmission) energy of

$$E_R \cong \left(\frac{2\pi}{w}\right)^2 + \frac{1}{2}Fw - \frac{4\pi^2 \sin^4(2\pi\varepsilon/w)}{w^2 \ln^2(\rho_0/R(\varepsilon))}. \tag{38}$$

In the case of a surface defect, i.e., when the atom is close to the wire's boundary (see **Appendix A**),

$$R(\varepsilon) \cong 4\varepsilon \exp(\gamma/2), \tag{39}$$

and then the zero-current energy is approximately

$$E_R \cong \left(\frac{2\pi}{w}\right)^2 + \frac{1}{2}Fw - \frac{\varepsilon^4(2\pi/w)^6}{\ln^2(\rho_0 \exp(-\gamma/2)/4\varepsilon)}. \tag{40}$$

Therefore, the zero-current energy has a linear dependence on the electric field (and thus on the applied external voltage). In **Figure 4** this property is presented by plotting the conductance for three different transverse electric fields.

6. The transistor working point

In **Figure 5,** the conductance as a function of the normalized applied electric field is plotted. The transistor can work as a digital device, where the field varies between the binary cases:

$$T_{1,1} = \begin{cases} 0 & for \quad F = F_R \\ 1 & for \quad F = 0 \end{cases} \tag{41}$$

where

$$\frac{1}{2}F_R w \equiv E_F - \left(\frac{2\pi}{w}\right)^2 + \frac{4\pi^2 \sin^4(2\pi\varepsilon/w)}{w^2 \ln^2(\rho_0/R(\varepsilon))} \cong E_F - \left(\frac{2\pi}{w}\right)^2 + \frac{\varepsilon^4(2\pi/w)^6}{\ln^2(\rho_0 \exp(-\gamma/2)/4\varepsilon)}. \tag{42}$$

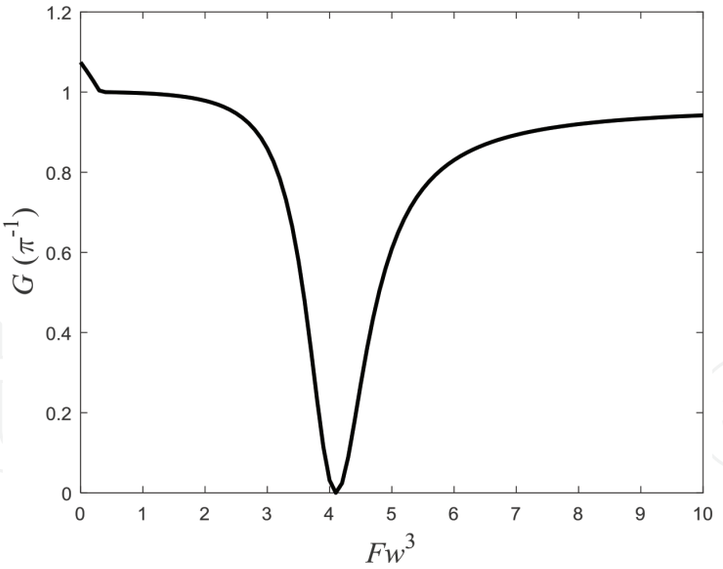


Figure 5.
Plot of the conductance as a function of the applied electric field for the particles' energy $E = 4(\pi/w)^2$.

But the transistor can also work in an analog mode as an amplifier, in which case the applied voltage should be modulated with respect to the bias voltage $F_* w$, which is the center of the linear regime, i.e.,

$$F_* w/2 = E_F - (2\pi/w)^2 + \delta^2 \left[1 \pm 2\frac{|\chi_1(\varepsilon)|^2}{|\chi_2(\varepsilon)|^2}\frac{\delta}{\sqrt{E_2 - E_1}}\right]. \tag{43}$$

Using this bias voltage, the transmission coefficient can be written

$$t_{1,1} = 1 - \left\{1 + ic\left[1 - \frac{\delta}{\sqrt{\delta^2/(1-c^{-1})^2 + (F - F_*)w/2}}\right]\right\}^{-1} \tag{44}$$

where
$c \equiv \frac{\sqrt{E_2 - E_1}}{\delta}\frac{|\chi_2(\varepsilon)|^2}{|\chi_1(\varepsilon)|^2} \cong 4\pi\sqrt{3}/\delta$, and $\delta \equiv \pi|\chi_2(\varepsilon)|^2/\ln(\rho_0/R(\varepsilon)) \cong 4\pi(2\pi\varepsilon)^2/[w^3 \ln(\rho_0 \exp(-\gamma/2)/4\varepsilon)]$.

Therefore, the transistor gain at the working point is the ratio between the change in conductance and the applied transverse voltage $\Delta v = (F - F_*)w$, which is

$$gain = \frac{\Delta G}{\Delta v} = \frac{c(1-c^{-1})^3}{4\pi\delta^2} \tag{45}$$

when the point defect is a surface one, i.e., $\varepsilon << 1$, then $\delta << 1$ and $c >> 1$

$$gain \cong \frac{\sqrt{3}}{\delta^3} = \frac{\sqrt{3}w^9 \ln^3(\rho_0 \exp(-\gamma/2)/4\varepsilon)}{(4\pi)^3(2\pi\varepsilon)^6}, \tag{46}$$

which can be extremely large.

7. Fast switching

When the dip of the resonances is very narrow, the gain is very high; however, in this case, the transistor response is very slow, because it takes a substantial

amount of time to establish the resonance. In fact, the gain is proportional to the transistor's time response τ, i.e.,

$$gain \propto \left(4\pi^2/w^2 - E\right)^{-1} \propto \tau. \tag{47}$$

However, the value of both can be controlled by changing the defect's parameters. Since

$$\rho_0 \cong 4\varepsilon \exp\left[\frac{\gamma}{2} + 2\pi \frac{\sin^2(2\pi\varepsilon/w)}{w\sqrt{4\pi^2/w^2 - E}}\right], \tag{48}$$

the parameter ρ_0 can be chosen to place the resonance dip at any point in the regime $\pi^2/w^2 < E < 4\pi^2/w^2$ and thus to determine the transistor time response

$$\rho_0 \cong 4\varepsilon \exp\left[\frac{\gamma}{2} + \frac{2\pi}{w} \sin^2(2\pi\varepsilon/w)\sqrt{\tau}\right]. \tag{49}$$

Therefore, the transistor with the quickest response is the one with a surface defect with

$$\rho_0 \cong 4\varepsilon \exp(\gamma/2). \tag{50}$$

In this case, the transistor time response is determined by the wire's width, i.e.,

$$\tau \sim (w/\pi)^2, \tag{51}$$

which in ordinary physical units is $\tau \sim m(w/h)^2$, i.e., the narrower the wire, the shorter the transistor's time response is.

Eq. (50) teaches that such a single-atom nanotransistor can be faster than any of the cutting-edge available transistors.

It should be emphasized that the point defect does not necessarily have to be an atom. It could be a molecule or any quantum dot that can be designed of having the necessary de-Broglie wavelength ρ_0.

8. Summary and conclusions

An innovative single-atom transistor configuration is suggested, which can be simplified and simulated by a simple model. The model consists of a narrow conducting wire, a single-point defect, and an electric field. This device's configuration does not require fine atomic-size gate contact and atomic-size accuracy for positioning the single atom. The device's mechanism is not based on resonant tunneling, and therefore, high accuracy is less essential. The gate is a capacitor that can be considerably larger than the point defect. Moreover, it was shown that this device can be extremely fast with a time response much shorter than any cutting-edge transistor.

The temporal analysis reveals a clear advantage of this configuration over resonant-tunneling ones (like [10, 14]). In resonant-tunneling devices, the signal's extinction ratio depends on the resonance state's lifetime. That is, there is no "zero-current" in resonant-tunneling devices. The minimum current ("zero") is actually a tunneling current, which is inversely proportional to the resonance state's lifetime. Therefore, in resonant-tunneling devices, "fast device" and "low minimum

current" are competing demands. When seeking the former, one has to compromise on the latter, and vice versa.

No such compromise is required in the proposed transistor configuration since it has been shown that this configuration always keeps (at least theoretically) extinction ratio of 100%.

A. Appendix A: derivation of Eq. (39)

The expression (26), i.e.,

$$R(\varepsilon) = \exp \lim_{\rho \to 0} \left[\ln \rho + \pi \sum_{q=3}^{\infty} \frac{\left|\chi_q(\varepsilon)\right|^2}{\sqrt{E_q - E}} \exp\left(-\left|E - E_q\right|\rho^2/4\right) \right]$$

as a function of the defect's location ε is plotted for several energy values in the energy range $\pi^2/w^2 < E < 4\pi^2/w^2$ in **Figure A1**.

As can be seen from this figure, while there are considerably large variations around $\varepsilon \cong 0.2$, the differences in the value of $R(\varepsilon)$ for $\varepsilon \cong 0.5$, i.e., when the defect is located at the center of the wire, are relatively mild, and in which case $R(\varepsilon) \cong 0.3$. Moreover, in the case of a surface defect, i.e., $\varepsilon << 1$, $R(\varepsilon)$ is independent of the particles' energy.

Using the definition $\xi \equiv \pi q \rho / w$ and the weak field approximation

$$\ln R(\varepsilon) \equiv \lim_{\rho \to 0} \left[\ln \rho + \frac{2}{w} \pi \exp\left(\pi^2 \rho^2 / w^2\right) \sum_{q=3}^{\infty} \rho \frac{\sin^2(\xi \varepsilon / \rho)}{\sqrt{\xi^2 - (4\pi\rho)^2 / w^2}} \exp\left(-\xi^2/4\right) \right] \tag{A1}$$

which can be written as an integral

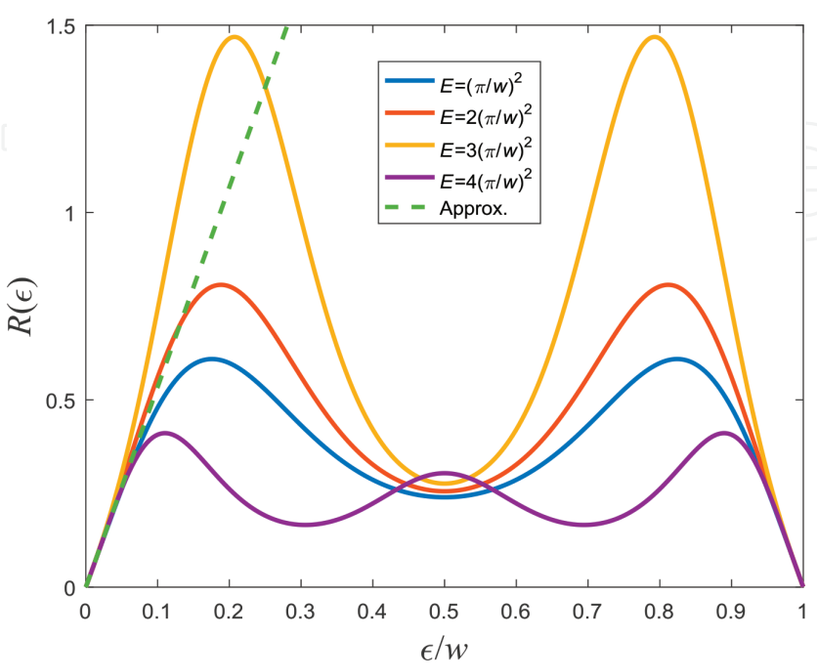


Figure A1.
Plots of $R(\varepsilon)$ as a function of the point defect's position in the wire ε for various energies. The dashed line is the small $\varepsilon/w << 1$ approximation (Eq. (39)).

$$\ln R(\varepsilon) \equiv \lim_{\rho\to 0}\left[\ln\rho + 2\int_{\pi 3\rho}^{\infty}\frac{\sin^2(\xi\varepsilon/\rho)}{\sqrt{\xi^2-(4\pi\rho)^2/w^2}}\exp\left(-\xi^2/4\right)d\xi\right]. \tag{A2}$$

And due to the limit,

$$R(\varepsilon) \cong \exp\lim_{\rho\to 0}\left[\ln\rho + 2\int_{0}^{\infty}\frac{\sin^2(\xi\varepsilon/\rho)}{\xi}\exp\left(-\xi^2/4\right)d\xi\right]. \tag{A3}$$

Now, since for $\rho/w << 1$

$$\ln(\rho/w) \cong \ln 2 - \gamma/2 - \int_{\rho/w}^{\infty}\frac{\exp\left(-\xi^2/4\right)}{\xi}d\xi, \tag{A4}$$

then

$$R(\varepsilon) \cong \exp\lim_{\rho\to 0}\left[\ln 2w - \gamma/2 - \int_{\rho/w}^{\infty}\frac{\exp\left(-\xi^2/4\right)}{\xi}d\xi + 2\int_{0}^{\infty}\frac{\sin^2(\xi\varepsilon/\rho)}{\xi}\exp\left(-\xi^2/4\right)d\xi\right] = \exp\lim_{\rho\to 0}\left[\ln 2w - \gamma/2 - \int_{\rho/w}^{\infty}\frac{\cos(2\xi\varepsilon/\rho)}{\xi}\exp\left(-\xi^2/4\right)d\xi + 2\int_{0}^{\rho/w}\frac{\sin^2(\xi\varepsilon/\rho)}{\xi}\exp\left(-\xi^2/4\right)d\xi\right]. \tag{A5}$$

Moreover, since, $\rho/\varepsilon \to 0$ but also $\varepsilon/w \to 0$, then in both integrals, the exponents can be ignored, i.e.,

$$R(\varepsilon) \cong \exp\lim_{\rho\to 0}\left[\ln 2w - \gamma/2 - \int_{\rho/w}^{\infty}\frac{\cos(2\xi\varepsilon/\rho)}{\xi}d\xi + 2\int_{0}^{\rho/w}\frac{\sin^2(\xi\varepsilon/\rho)}{\xi}d\xi\right] \tag{A6}$$

which finally yields the analytical expression

$$R(\varepsilon) \cong \exp\left[\ln 2w - \gamma/2 + \mathrm{Ci}(2\varepsilon/w) + \varepsilon^2/w^2\right] = 4\varepsilon\exp\left(\frac{\gamma}{2}\right), \tag{A7}$$

where Ci(x) is the cosine integral function [22].

Author details

Er'el Granot
Department of Electrical and Electronics Engineering, Ariel University, Ariel, Israel

*Address all correspondence to: erel@ariel.ac.il

IntechOpen

© 2018 The Author(s). Licensee IntechOpen. This chapter is distributed under the terms of the Creative Commons Attribution License (http://creativecommons.org/licenses/by/3.0), which permits unrestricted use, distribution, and reproduction in any medium, provided the original work is properly cited. CC BY

References

[1] Moore G. Chapter 7: Moore's law at 40. In: Brock D, editor. Understanding Moore's Law: Four Decades of Innovation. Philadelphia, PA: Chemical Heritage Foundation; 2006. pp. 67-84

[2] Takahashi D. Forty Years of Moore's Law. San Jose, CA: Seattle Times; 2005

[3] Eigler DM, Schweizer EK. Positioning single atoms with a scanning tunnelling microscope. Nature. 1990; **344**:524-526

[4] Koenraad PM, Flatté ME. Single dopants in semiconductors. Nature Materials. 2011;**10**:91-100

[5] Lansbergen GP et al. Gate-induced quantum-confinement transition of a single dopant atom in a silicon FinFET. Nature Physics. 2008;**4**:656-661

[6] Calvet LE, Snyder JP, Wernsdorfer W. Excited-state spectroscopy of single Pt atoms in Si. Physical Review B. 2008; **78**:195309

[7] Tan KY et al. Transport spectroscopy of single phosphorus donors in a silicon nanoscale transistor. Nano Letters. 2010;**10**:11-15

[8] Hollenberg LCL et al. Charge-based quantum computing using single donors in semiconductors. Physical Review B. 2004;**69**:113301

[9] Schofield SR et al. Atomically precise placement of single dopants in Si. Physical Review Letters. 2003;**91**: 136104

[10] Fuechsle M, Miwa JA, Mahapatra S, Ryu H, Lee S, Warschkow O, et al. A single-atom transistor. Nature Nanotechnology. 2012;**7**:242-246

[11] Xie F-Q, Maul R, Wenzel W, Schn G, Obermair Ch, Schimmel Th. Single-atom transistors: Atomic-scale electronic devices in experiment and simulation. In: Proceedings of the International Beilstein Symposium on Functional Nanoscience; May 2010. pp. 213-228

[12] Fuechsle M, Miwa JA, Mahapatra S, Warschkow O, Hollenberg LCL, Simmons MY. Realisation of a single-atom transistor in silicon. Journal and Proceedings of the Royal Society of New South Wales. 2012;**145**(443 & 444): 66-74

[13] Obermair C, Xie F-Q, Schimmel T. The single-atom transistor: Perspectives for quantum electronics on the atomic-scale. Europhysics News. 2010;**41**:25-28

[14] Granot E. Exact model for single atom transistor. In: Stavrou VN, editor. Nonmagnetic and Magnetic Quantum Dots. Rijeka, Croatia: IntechOpen; 2018. Chapter 1

[15] Granot E, Azbel MY. Resonant angular dependence in a weak magnetic field. Journal of Physics: Condensed Matter. 1999;**11**:4031

[16] Granot E, Azbel MY. Resonant tunneling in two dimensions via an impurity. Physical Review B. 1994;**50**: 8868

[17] Granot E. Universal conductance reduction in a quantum wire. Europhysics Letters. 2004;**68**:860-866

[18] Miroshnichenko AE, Flach S, Kivshar YS. Fano resonances in nanoscale structures. Reviews of Modern Physics. 2010;**82**:2257-2298

[19] Azbel MY. Variable-range-hopping magnetoresistance. Physical Review B. 1991;**43**:2435

[20] Azbel MY. Quantum particle in a random potential: Implications of an

exact solution. Physical Review Letters. 1991;**67**:1787

[21] Granot E. Point scatterers and resonances in low number of dimensions. Physica E. 2006;**31**:13-16

[22] Abramowitz M, Stegun IA. Handbook of Mathematical Functions. New York: Dover Publications; 1972

[23] Granot E. Transmission coefficient for a point scatterer at specific energies is affected by the presence of the scatterer but independent of the scatterer's characteristics. Physical Review B. 2005;**71**:035407

[24] Granot E. Symmetry breaking and current patterns due to a weak imperfection. Physical Review B. 2000; **61**:11078

[25] Landauer R. Spatial variation of currents and fields due to localized scatterers in metallic conduction. IBM Journal of Research and Development. 1957;**1**:223-231

[26] Nazarov YV, Blanter YM. Quantum Transport: Introduction to Nanoscience. Cambridge, UK: Cambridge University Press; 2009. pp. 29-41